A simplified model of the back surface of a charge-coupled device*

Morley M. Blouke
Tektronix Inc.
Beaverton OR, 97077

and

W.A. Delamere and G. Womack
Ball Aerospace Systems Division
Boulder CO, 80306

Abstract

A simplified model of the back surface of the CCD is discussed. The model incorporates parameters which account for the important features of the back surface: a surface recombination velocity, an electric field which can assist in or oppose the collection of signal charge and a field free region. Calculations using the model equations are presented to illustrate the effect of these parameters on the distribution of excess carriers and on the resulting quantum efficiency. The results indicate that only moderate fields are required to achieve high quantum efficiencies even at short wavelengths.

1. Introduction

One of the great advantages of the charge-coupled device (CCD) as a detector is the possibility of achieving very high quantum efficiencies over a broad range of wavelengths. The highest sensitivities are achieved by thinning the device and illuminating from the non-circuit side. In this manner and in combination with appropriate anti-reflection coatings, it is possible to obtain quantum efficiencies that exceed 90% at the peak.

Thinning of CCD devices has been a subject of intense interest for a number of years. It was recognized very early that to achieve respectable response at short wavelengths (k < 450 nm) it would be necessary to illuminate the device from the non circuit side. Many of the early devices used either an all aluminum gate technology or polysilicon gate technology [1,2]. In the case of the Al gate devices it was clear that to get light into the device it was necessary to bring light in from the back side. In the case of the polysilicon devices the problem is the polysilicon gates themselves. Figure 1 illustrates the absorption coefficient of Si as a function of wavelength. For wavelengths shorter than about 450 nm the polysilicon gates themselves will absorb a significant fraction of the incident radiation resulting in low quantum efficiency in the short wavelength region.

For the rear illuminated devices, the same figure indicates that for short wavelengths the photo-generated electrons will be generated very close to the back surface of the device. The consensus is that trapped charge in the native oxide that typically grows on the back surface creates a potential well extending several hundred nm into the silicon. Figure 2 presents a schematic cross section of a thinned CCD and illustrates the presence of the potential well at the back surface. The net effect of

* This work performed for Ball Aerospace Systems Division under contract No. 02744 in support of the NASA Space Telescope Imaging Spectrograph (STIS) Program.

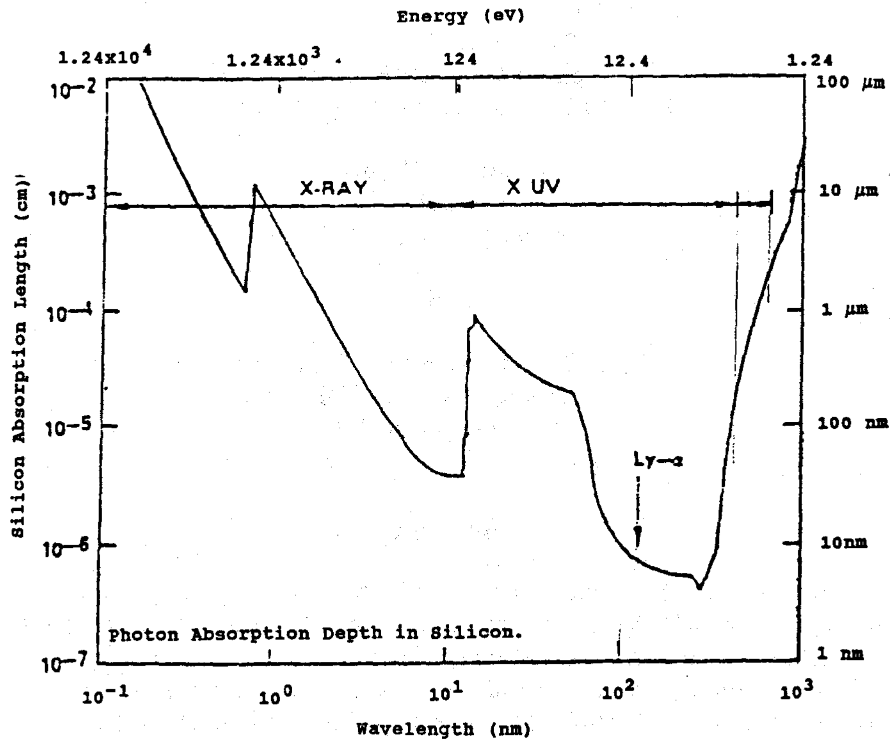

Fig. 1. Absorption length in silicon.

this potential well is to attract photo-generated electrons to the back surface where they will recombine and be unable to contribute to the signal. The result is a lower effective quantum efficiency. It is, of course, the short wavelength photons which suffer the greatest degradation. Consequently, care must be exercised in treating the back surface of the device in order to ensure that the largest fraction of these signal carriers are in fact collected and detected.

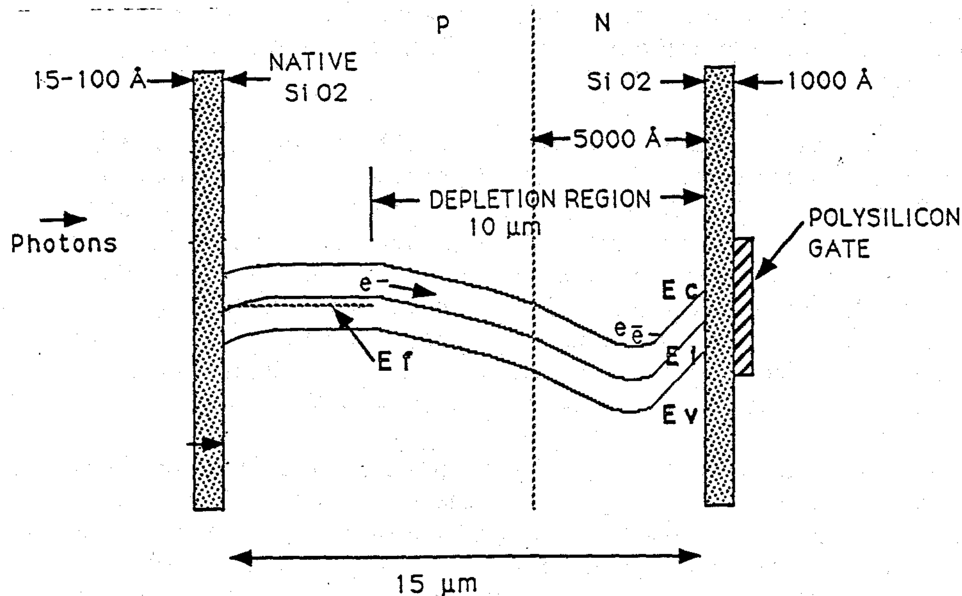

Fig. 2. Schematic cross section of a thinned CCD. The depletion region at the back surface leads to poor quantum efficiency at short wavelengths.

A number of efforts to computer model the thinned CCD have been made [3-5]. These models simulate the drift and diffusion of carriers in the surface and field free regions and allow one to evaluate both charge collection efficiency and the distribution of charges over pixels for high energy events. Although the computer models have proven useful and reliable in predicting results, an analytical solution generally gives more insight into the physics of the problem. Furthermore, with an analytical model it is usually easier to evaluate the influence of individual parameters of the overall performance of the structure. In this paper we will present a simple model of the back surface of the CCD which includes the effects of surface recombination, a surface potential well and a field free region.

2. Simplified Model

A number of different techniques have been devised in the effort to treat the back surface of a thinned devices so as to achieve the highest quantum efficiency possible. The original method, and the one which illuminated the underlying problem with the bare Si surface, was the technique of UV flooding [6]. Since that time a number of other processes have been developed including charging the back surface, flash oxides, biased flash gates and ion implanting and annealing [3,7,8]. The common feature of all these techniques is the effort to mitigate, compensate, or eliminate the potential well that forms naturally on the back surface. In general this is accomplished by creating a field in the surface region which will bend the bands upwards, accumulating the surface. This field is in such a direction as to accelerate photo-generated electrons towards the CCD wells and away from the back surface.

The simplified model begins with the assumptions that the neutral bulk region of the thinned device contains both a field free region and region next to the surface that involves a field of some sort [9]. In addition, the surface is assumed to have a finite, nonzero surface recombination velocity which provides the natural sink for electrons that diffuse towards the surface. Figure 3 is a schematic illustration of the regions of a thinned CCD of total thickness t. Also presented in the figure are the potential and the electric field as a function of position. We assume the region of the surface which includes the field is characterized by a distance into the silicon, σ, and a constant field, E_0. The field represents the effects the charge in the native oxide and/or band bending (independent of how the band bending is implemented). The field can be positive or negative corresponding to a depleted or an accumulated surface, respectively. The field free region extends from σ to d, the edge of the depletion region. Finally, the depletion region and the CCD well comprise the remainder of the structure, $d < x < t$. The back surface is characterized by the surface recombination velocity, s_0.

To evaluate the quantum efficiency of the back illuminated device we need to calculate the flux of photo generated electrons that are collected by the CCD wells and add to that the number of carriers that are generated directly in the CCD wells. Mathematically this is expressed as

$$QE(\lambda) = (1 - R(\lambda)) \{ \int_d^t G_n(x)dx - (1/q)\, J_n(x=d)\}/\phi_0 \qquad (1)$$

where $R(\lambda)$ is the fraction of the incident energy reflected from the thinned surface, $G_n(x)$ is the generation rate and $J_n(x)$ is the electron current in the field free region evaluated at the edge of the depletion region and ϕ_0 is the incident photon flux.

The electron current can be found from the solution to the continuity equation in the neutral bulk for the electron concentration, n(x),

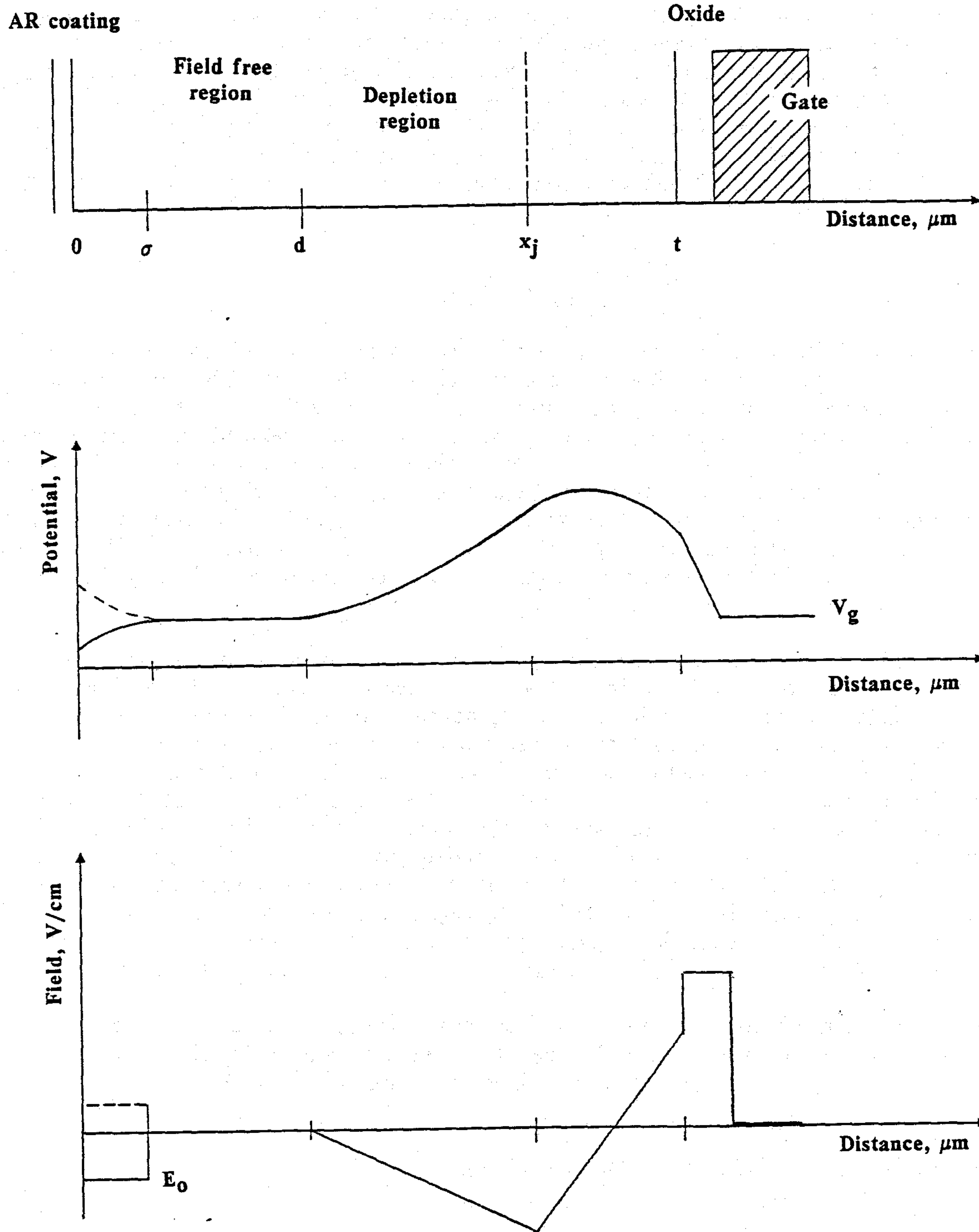

Fig. 3. Cross section of the model for the back surface of the CCD. Top: Illustration of the individual regions into which the device is segmented. These include the surface region, the field free region and the depletion and CCD well region. Middle: Potential profile within the device. Note that the potential at the surface can bend upwards or downwards representing inversion or accumulation, respectively. Bottom: Fields present within the device. The field can be either positive or negative.

$$\partial n/\partial t = (1/q)\ \nabla \cdot J_n(x) + G_n(x) - R_n \tag{2}$$

$$= \mu_n n(x)\ dE(x)/dx + \mu_n E(x)\ d\delta n(x)/dx + D_n\ d^2\delta n(x)/dx^2 + G_n(x) - R_n \tag{3}$$

In these expressions, q is the magnitude of the electronic charge, R_n is the electron recombination rate, μ_n is the electron mobility, E(x) is the electric field, D_n is the electron diffusion constant and $n(x) = n_o(x) + \delta n(x) \approx \delta n(x)$.

For the optical problem,

$$G_n(x) = \alpha\phi_o \exp(-\alpha x) \tag{4}$$

and

$$R_n = \delta n(x)/\tau \tag{5}$$

where α is the absorption coefficient and τ is the recombination lifetime. The last condition reflects the fact that the electrons are the minority carrier in the bulk and it is the excess minority carriers that are collected as signal. In the steady state, $\partial n/\partial t = 0$, and the continuity equation must be solved for two regions: the surface region, region 1, where the electric field is assumed to be uniform, $E(x) = E_o$ and the field free region, layer 2, where $E(x) = 0$. The solution in the two regions are

$$\delta n_1(x) = A \exp(\mu x) + B \exp(\nu x) + \psi \exp(-\alpha x) \qquad 0 < x \le \sigma \tag{6}$$

and

$$\delta n_2(x) = A \exp(\gamma x) + B \exp(-\gamma x) + \xi \exp(-\alpha x) \qquad \sigma < x \le d \tag{7}$$

The coefficients A - D are determined from the boundary conditions. The detailed solution, the coefficients and other constants are given in Appendix A. Substituting the expression for the excess electron concentration into Eq. (1), the result for the quantum efficiency as a function of wavelength is

$$QE(\lambda) = (1 - R(\lambda))\{ (\exp(-\alpha d) - \exp(-\alpha t) + D_n [\ \gamma\ D(\lambda) \exp(-\gamma d) + \xi(\lambda)\ \alpha \exp(-\alpha d) - \gamma\ C(\lambda) \exp(\gamma d)\ ]\ \}/\phi_o \tag{8}$$

3. Model Calculations

Equations (6), (7) and (8) can now be used to explore the effect of the condition of the back surface of the CCD on the electron distribution and on the quantum efficiency. In particular, we can now begin to investigate the effects of the electric field that can be built into the surface and the surface recombination velocity. One of the major techniques of interest in treating the back surface is ion implantation and laser annealing. If one assumes a boron implant with a laser anneal, the resultant distribution has a roughly Gaussian profile. One can now make an estimate of the field. Assume that the impurity profile is given by

$$q_A = A\exp(-x^2/\sigma^2) + N_A \tag{9}$$

and the field is given by

$$E(x) = (kT/q)\ d(\ln(q_A))/dx \tag{10}$$

$$= -(2kTx/q\sigma^2)(A\exp(-x^2/\sigma^2)/q_A) \tag{11}$$

Figure 4 presents a graph of E(x) and q_A for a typical ion implantation dose and straggle of the parameters and shows the value of the field that might be expected. It is clear that the field is not

constant. It should be pointed out that Eq. (11) is valid as long as the quasi-neutrality condition obtains. In the model, E_0 is taken as an average field that spans the region of interest. Note that the field is negative indicating that electrons will be driven towards the CCD wells.

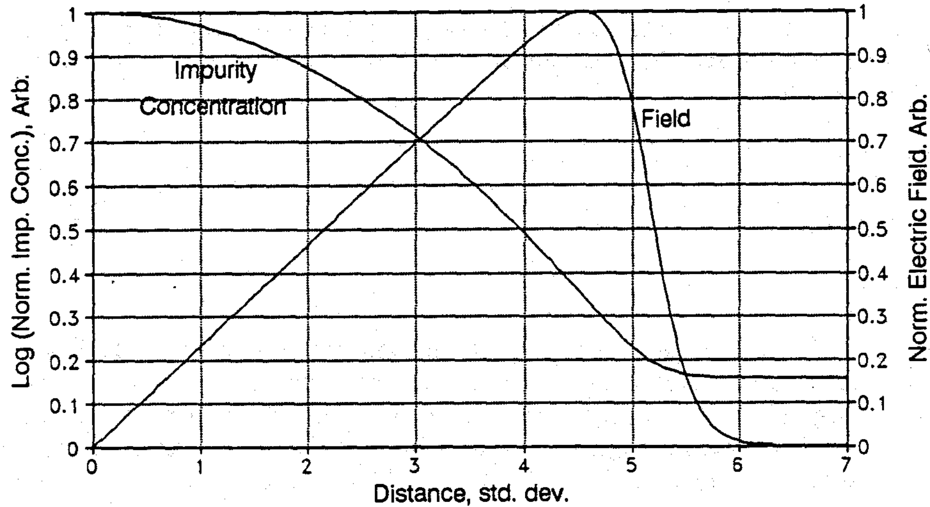

Fig. 4. Graph of the normalized impurity concentration and the normalized field due to the impurity gradient as a function of the standard deviation of the impurity distribution. The magnitude of the field at the peak, assuming quasi-neutrality, can be > 10^5 V/cm.

The effect of the surface recombination velocity on the electron distribution in the absence of any extraneous electric field can be used as a check on the validity of the solution obtained above. The results of calculations using Eqs. (6) and (7) are shown in Fig. 5. In the figure the normalized excess carrier concentration is presented as a function of position with surface recombination velocity as the parameter. The thickness of the undepleted region in the neutral bulk is assumed to be 5 μm and the excess carrier concentration is forced to zero at the edge of the depletion region. A wavelength of 600 nm was chosen which will result in some generation throughout the field free region. For $s_0 = 0$ cm/sec the slope of the carrier concentration curve at the surface is zero indicating that the surface has no influence on the distribution.

This does not imply that all the carriers will be collected because normal recombination takes place within the field free region; however, we are not losing any signal electrons to the surface. Low values of s_0 (< 10^3 cm/sec) do not affect the distribution significantly. A fresh, clean surface will have a surface recombination velocity of between 10^2 and 10^3 cm/sec [10,11]. Values of s_0 between 10^4 and 10^6 have, however, a significant effect on the distribution.

The normal thinned surface is assumed to have a native oxide a depletion layer associated with it. In this model such a depletion layer is treated as a positive field acting over some distance, σ. Figure 6 illustrates the results of calculations assuming a field of $E_0 = +10^3$ V/cm and $\sigma = 200$ nm. The values of the surface recombination velocity are the same as used to generate the curves in Fig. 5. Two features are to be noted. First there is an accumulation of electrons at the surface. The field is driving the photo-generated carriers towards the surface where they will recombine. Secondly, if one compares the distributions for the same surface recombination velocity, the concentration in the field free region is lower in every case. This will result in fewer carriers being collected and a lower quantum efficiency.

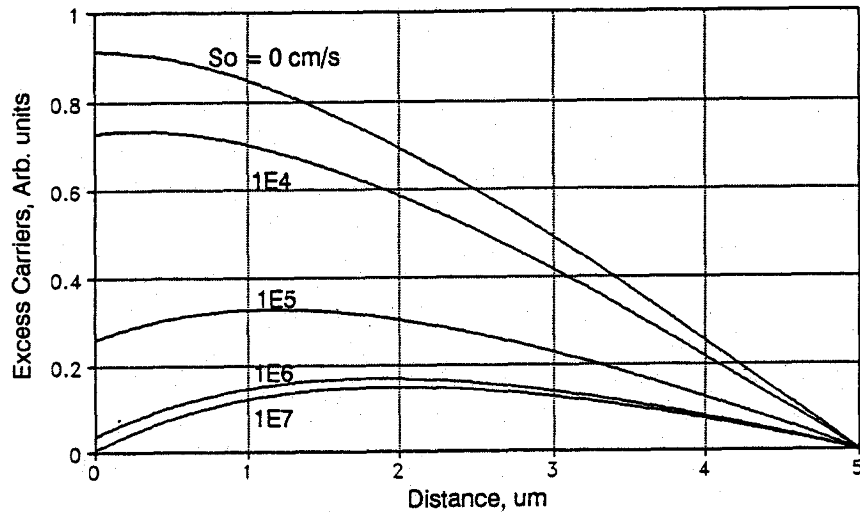

Fig. 5. Excess carrier concentration as a function of distance into the CCD for various values of the surface recombination velocity. Conditions are: t = 20 μm, d = 5 μm, E_o = 0 V/cm, λ = 600 nm and σ = 0 μm.

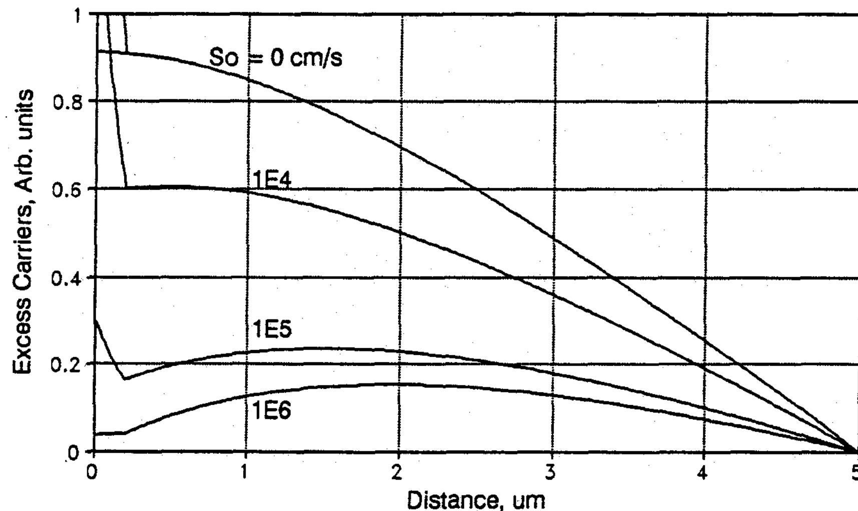

Fig. 6. Excess carrier concentration as a function of distance for selected values of the surface recombination velocity. Conditions are: t = 20 μm, d = 5 μm, E_o = +10^3 V/cm, λ = 600 nm and σ = $2x10^{-5}$ cm

Figures 7 and 8 illustrate the effect of a negative field on the distribution. The negative field is in such a direction to force carriers away from the surface preventing them from recombining there. This is the behavior we are anticipating and desire for an accumulated surface. Figure 7 illustrates the condition assuming a field of -10^3 V/cm and various surface recombination velocities. The curve for s_o = 0 is the same as in Fig. 5. We note that for equivalent values of s_o the distribution in the field free region is increased and the surface concentration is lower. This reflects the fact that the field is driving carriers away from the surface into the field free region. These effects are enhanced in Fig. 7 where we have assumed a field of E_o = -$5x10^3$ V/cm. Note in this figure that the distribution for s_o = 10^4 cm/sec is virtually identical to the curve for s_o = 0 except in the surface region. In Fig. 6-8, the discontinuity in the slope of the carrier distribution at x = σ is artificial and is, of course, the result of assuming that the field drops abruptly to 0 at that point.

It should be noted that a moderate field (-$5x10^3$ V/cm) acting over a distance of 200 nm effectively eliminates any effect of surface recombination for values of s_o less than about 10^5 cm/sec.

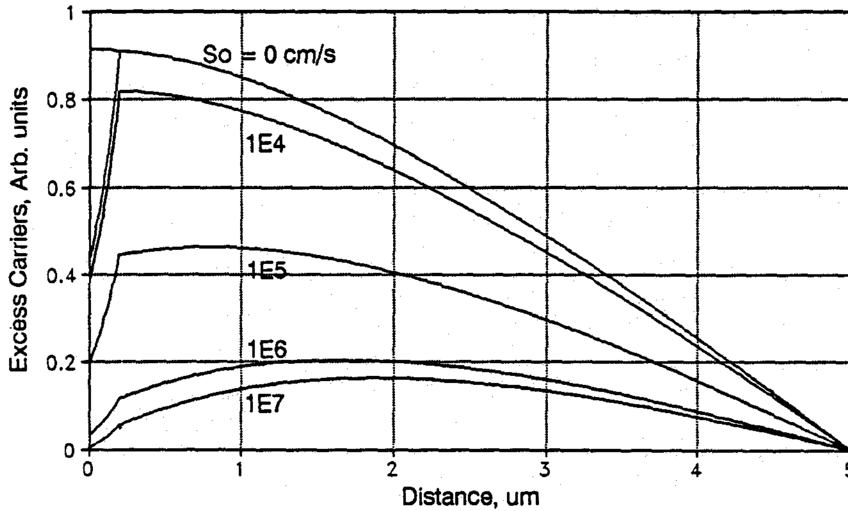

Fig. 7. Excess carrier concentration as a function of distance for selected values of the surface recombination velocity. Conditions are: t = 20 μm, d = 5 μm, $E_0 = 10^3$ V/cm, λ = 600 nm and $\sigma = 2x10^{-5}$ cm.

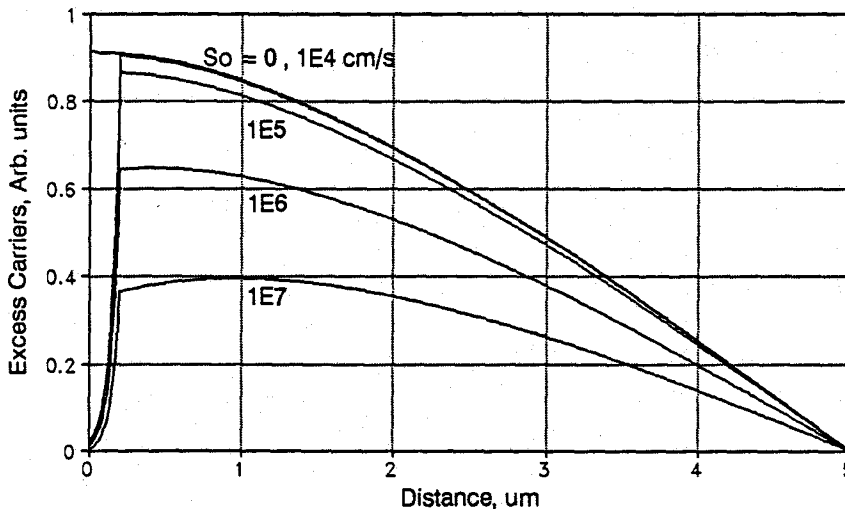

Fig. 8. Excess carrier concentration as a function of distance for selected values of the surface recombination velocity. Conditions are: t = 20 μm, d = 5 μm, E_0 = -5x10^3 V/cm, λ = 600 nm and $\sigma = 2x10^{-5}$ cm.

Using Eq. (9), the model has be employed to explore the effects of various surface recombination velocities and field/distance combinations on quantum efficiency. Figure 9 presents calculated curves of quantum efficiency as a function of wavelength for different surface recombination velocities. In the calculations it was assumed that the built-in electric field in the surface region is E_0 = +10^3 V/cm, the same as was assumed for the calculations of Fig. 6. The curve of quantum efficiency for s_0 = 0 is limited at short wavelengths by reflection losses and agrees with previous calculations of the quantum efficiency [12]. This is as good as one can do. At longer wavelengths some photons pass thru the device and consequently can not contribute to the QE. As is expected, the quantum efficiency drops as the surface recombination velocity increases. This is consistent with photo-generated carriers being attracted to the back surface and recombining there. Furthermore, the effect is much more dramatic for short wavelengths than for wavelengths longer than 800 nm. Again, this is the expected result since for short wavelengths, as noted in the introduction, most of the carriers are generated near the surface. For s_0 = 10^6 cm/sec the response at 800 nm is respectable while the response at 400 has practically been eliminated.

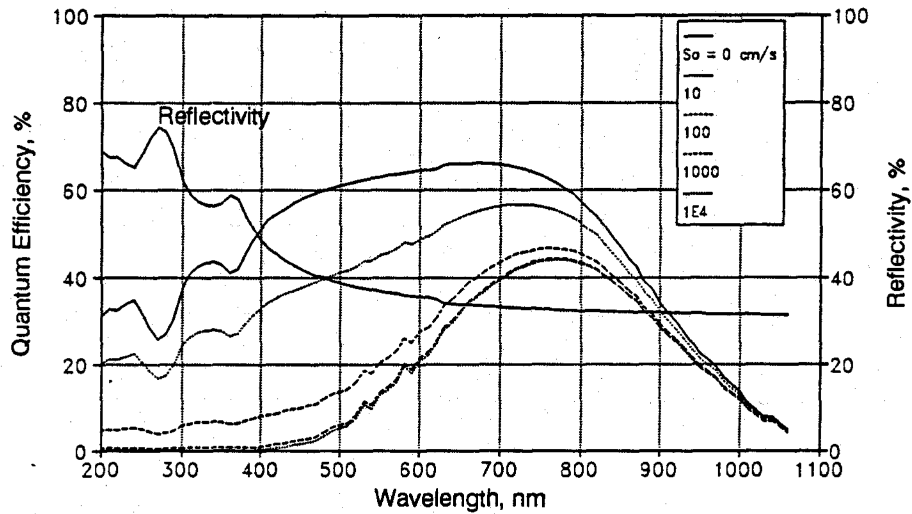

Fig. 9. Theoretical curves of quantum efficiency as a function of wavelength for various surface recombination velocities. The conditions for the calculations are: $t = 20\ \mu m$, $d = 5\ \mu m$, $E_0 = +10^3$ V/cm, $\lambda = 600$ nm and $\sigma = 2x10^{-5}$ cm.

The effects of a negative field are investigated in Fig. 10. For these calculations the surface region was assumed to be a region 50 nm wide. This is the situation one might expect for a very shallow B implant and laser anneal. The surface recombination velocity of 10^7 cm/sec was used for the calculations. As shown in the figure, to achieve a quantum efficiency that is limited by the reflection losses requires a field of $-5x10^4$ V/cm. The higher field is required in these calculations because the field is effective over a shorter distance. This effect is illustrated in Fig. 11 where the variation in the quantum efficiency with the thickness of the surface region is investigated. The range of values for σ extends from 10 to 100 nm while the quantum efficiency at 400 nm increases from 1% to 50%..

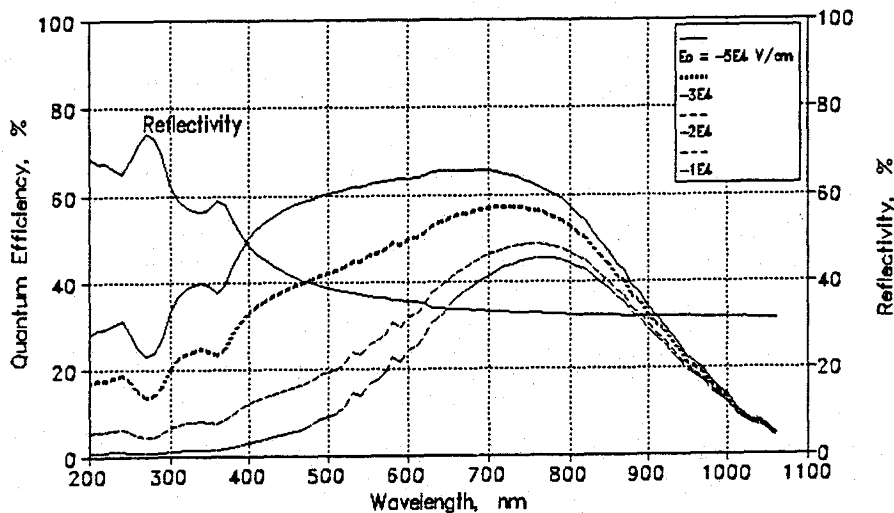

Fig. 10. Theoretical curves of quantum efficiency as a function of wavelength for various negative fields in the surface region. The conditions are: $t = 20\ \mu m$, $d = 5\ \mu m$, $s_0 = +10^7$ cm/sec, $\lambda = 600$ nm and $\sigma = 5x10^{-6}$ cm.

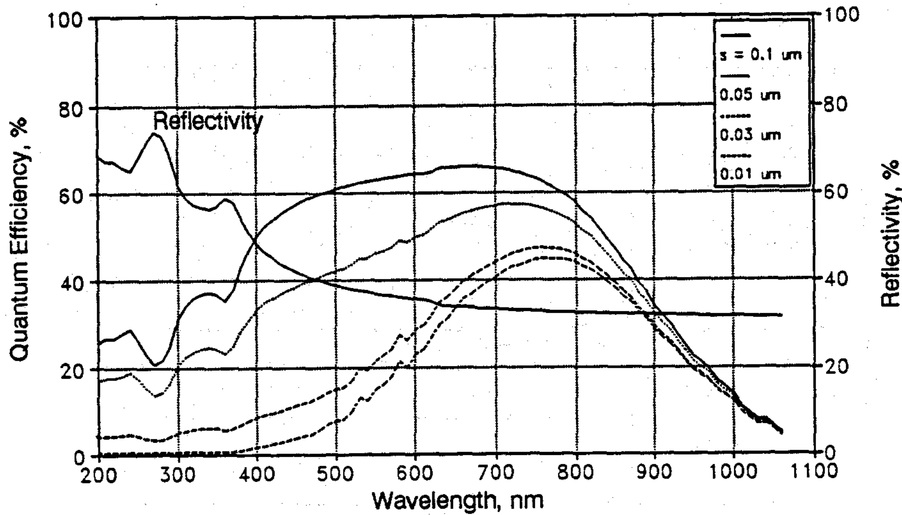

Fig. 11. Theoretical curves of quantum efficiency as a function of wavelength for selected values of the width of the surface region. The conditions are: $t = 20\ \mu m$, $d = 5\ \mu m$, $E_0 = +10^4$ V/cm, $\lambda = 600$ nm and $s_0 = 10^7$ cm/sec.

4. Experimental Results

The model has been used to perform a preliminary fit to the data for a device which was thinned and which received the standard back surface enhancement treatment and standard anti-reflection coating. The results of the fit and the data are shown in Fig. 12. The agreement is very good assuming $E_0 = -3\text{x}10^3$ V/cm, $s_0 = 4\text{x}10^4$ cm/sec and $\sigma = 80$ nm. These are all reasonable values for these parameters.

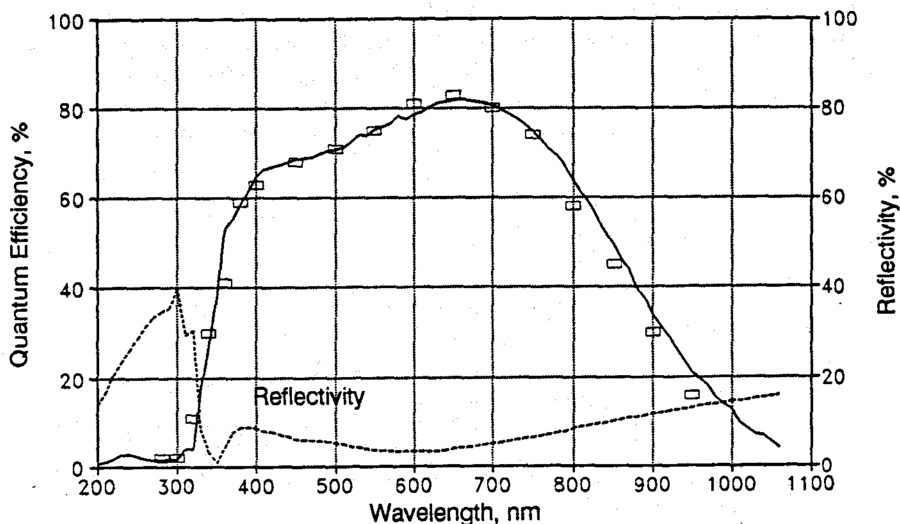

Fig. 12. Measured values of the quantum efficiency for a device which had received a back surface enhancement treatment and an AR coating. The solid curve is the theoretical curve based on Eq. (9).

5. Summary

A simplified model for the quantum efficiency of the back surface of a thinned charge-coupled device has been developed. The model is based on our current understanding of physics of what is happening at the back surface and attempts to include the important features of the back surface in a

closed form solution. The CCD is divided into three regions: the surface region, the CCD well and depletion region and a field free region which lies between the two. The simplifying assumption that permits a closed form solution is to treat the surface region as a thin region with a constant electric

field. Any technique that is employed to enhance the back surface of the CCD whether it be a surface charging or an ion implantation will produce an internal electric field. Typically this field will be non uniform. In the model this complex field is represented by an average value which is assumed to be effective over some characteristic distance. This assumption makes possible a simple solution to the continuity equation that governs the distribution of excess carriers in the neutral bulk of the device. The other important parameters included in the model are the surface recombination velocity, which depends upon the details of the treatment of the back surface, and the electron mobility and lifetime. Finally, the thickness of the depletion region and the thickness of the thinned device are also included.

Calculations of the excess carrier concentration using the model equations show exactly the behavior that would be expected. For positive fields, which represent depletion of the back surface, we find that the distribution of excess carriers shows an enhancement near the surface. Negative fields which drive photo generated electrons towards the depletion regions produce distributions which clearly show a deficit near the surface. Model calculations of the quantum efficiency show that large surface recombination velocities significantly degrade the QE as does a positive field in the surface region. The interesting observation is that only modest fields acting over tens to hundreds of nm are required to ameliorate the effects of the surface recombination velocity.

Although much work remains to be done, preliminary fits of the model to real data of an enhanced and AR coated device show promise. These efforts will be reported at a later time.

6. Acknowledgments

The authors would like to D.L. Heidtmann and L.D. Riley for many helpful discussions and continuing support.

Appendix A

The model begins with the continuity equation for electrons which must be solved in each of the two regions (see Fig.

$$\partial n/\partial t = (1/q)\ \nabla \cdot J_n(x) + G_{nn}(x) - R_{nn} = 0 \tag{A1}$$

The electron current is

$$J_n n(x) = \mu_n n(x)\ E(x) + D_n\ dn(x)/dx \tag{A2}$$

$$= \mu_n n(x)\ dE(x)/dx + \mu_n E(x)\ d\delta n(x)/dx + D_n\ d^2\delta n(x)/dx^2 + G_n(x) - R_n \tag{A3}$$

The generation rate and the recombination rate are given by

$$G_n = \alpha\phi_o\ \exp(-\alpha x) \tag{A4}$$

$$R_n = \delta n(x)/\tau \tag{A5}$$

where α is the wavelength dependent absorption coefficient, ϕ_o is the flux on the device and τ is the recombination lifetime.

The continuity equation must then be solved for two regions: the surface region, region 1, where the electric field $E(x) = E_O$ and the field free region, region 2, where $E(x) = 0$. The equations we need to solve are:

$$d^2\delta n(x)/dx^2 + (\mu_n/D_n)\, E_O\, d\delta n(x)/dx - \delta n(x)/(D_n\tau) = -\,\alpha\phi_O \exp(-\alpha x)/D_n \qquad 0 < x < \sigma \qquad (A6)$$

and

$$d^2\delta n(x)/dx^2 - \delta n(x)/(D_n\tau) = -\,\alpha\phi_O \exp(-\alpha x)/D_n \qquad \sigma < x < d \qquad (A7)$$

The boundary conditions are:

$$x = 0: \qquad (1/q)J_1(x{=}0) = s_O\, \delta n_1(x{=}0) \qquad (A8)$$

or

$$d\delta n_1(x)/dx = ((s_O - \mu_n E_O)/D_n)\, \delta n_1(x{=}0) \qquad (A9)$$

$$x = x_d: \qquad \delta n_2(x{=}x_d) = 0 \qquad (A10)$$

The first condition, Eq. (9), accounts for the physical condition of the back surface through the surface recombination velocity. Equation (A10) reflects the requirement that if the electrons get to the depletion edge they get collected in the CCD well. In addition, at

$$x = \sigma: \qquad \delta n_1(x{=}\sigma) = \delta n_2(x{=}\sigma) \qquad (A11)$$

and

$$J_n(x{=}\sigma) = J_n(x{=}\sigma) \qquad (A12)$$

or

$$\mu_n E_O\, \delta n_1(x{=}\sigma) + D_n d\delta n_1(x{=}\sigma)/dx = D_n d\delta n_2(x{=}\sigma)/dx \qquad (A13)$$

The last two conditions state that the electron concentration and the electron current must be continuous between regions 1 and 2.

The solutions for the two regions are

$$\delta n_1(x) = A \exp(\mu x) + B \exp(\nu x) + \psi \exp(-\alpha x) \qquad 0 < x < \sigma \qquad (A14)$$

and

$$\delta n_2(x) = C \exp(\gamma x) + D \exp(-\gamma x) + \xi \exp(-\alpha x) \qquad \sigma < x < x_d \qquad (A15)$$

where

$$\mu,\nu = -\beta \pm \sqrt{(\beta^2 + \gamma^2)} \qquad (A16)$$

$$\beta = (\mu_n E_O/(2D_n)) = (qE_O/(2kT)) \qquad (A17)$$

$$\gamma = 1/L_n = 1/\sqrt{(D_n\tau)} \qquad (A18)$$

$$\psi = (\alpha\phi_O)/(D_n(\gamma^2 + 2\alpha\beta - \alpha^2)) \qquad (A19)$$

$$\xi = (\alpha\phi_O)/(D_n(\gamma^2 - \alpha^2)) \qquad (A20)$$

and

$$\eta = -(s_O/D_n - 2\beta). \qquad (A21)$$

Applying the boundary conditions one arrives at the solutions for the constants:

$$B= \xi \{ [(\alpha-2\beta)\exp(-\alpha\sigma) + \nu((\nu+\eta)/(\mu+\eta))\exp(\mu\sigma)] \sinh(\gamma(d-\sigma)) \}/X +$$

$$- \xi \{ \gamma[\exp(-\alpha\sigma) + ((\alpha-\eta)/(\mu+\eta))\exp(\mu\sigma)] \cosh(\gamma(d-\sigma)) \}/X +$$

$$+ \psi \{ \gamma[\exp(-\alpha\sigma) - \exp(\gamma\sigma)\exp(-(\alpha+\gamma)d)] \cosh(\gamma(d-\sigma)) \}/X +$$

$$- \psi \{ [\alpha\exp(-\alpha\sigma) + \gamma\exp(\gamma\sigma)\exp(-(\alpha+\gamma)d)] \sinh(\gamma(d-\sigma)) \}/X, \qquad (A22)$$

where

$$X = \{ \gamma[\exp(\nu\sigma) - ((\nu+\eta)/(\mu+\eta))\exp(\mu\sigma)] \cosh(\gamma(d-\sigma)) +$$

$$- [\mu\exp(\nu\sigma) - \nu((\nu+\eta)/(\mu+\eta))\exp(\mu\sigma)] \sinh(\gamma(d-\sigma))\}. \qquad (A23)$$

Similarly,

$$D = B \{\exp(\nu\sigma) - ((\nu+\eta)/(\mu+\eta))\exp(\mu\sigma)\}/(2\exp(-2\gamma d)\sinh(\gamma(d-\sigma))) +$$

$$\xi \{\exp(-\alpha\sigma) + ((\alpha-\eta)/(\mu+\eta))\exp(\mu\sigma)\}/(2\exp(-2\gamma d)\sinh(\gamma(d-\sigma))) +$$

$$- \psi \{\exp(-\alpha\sigma) - \exp(\gamma\sigma)\exp(-(\alpha+\gamma)d)\}/(2\exp(-2\gamma d)\sinh(\gamma(d-\sigma))) \qquad (A24)$$

$$C = - D \exp(-2\gamma d) - \xi \exp(-(\alpha+\gamma)d) \qquad (A25)$$

$$A = \psi ((\alpha-\eta)/(\mu+\eta)) - B ((\nu+\eta)/(\mu+\eta)) \qquad (A26)$$

References

1. Collins, D.R., S.R. Shortes, W.R. McMahon, R.C. Bracken and T.C. Penn, "Charge-coupled devices fabricated using aluminum-anodized aluminum-aluminum double level metallization," *J. Electrochem. Soc.*, 120, 521-526 (1973).

2. Rodgers, R.L. III, "Charge-coupled imager for 525-line television," Proc. 1974 IEEE Int. Conv. and Exposition, Tech. Digest of Papers (Mar. 1974) pp 1-4.

3. Janesick, J.R., T. Elliott, T. Daud and D. Campbell, "The CCD flash gate," in *Instrumentation in Astronomy, VI* (Ed. D. Crawford), Proc. SPIE 982, 543-582 (1986).

4. Hopkinson, G.R., "Analytic modeling of charge diffusion in charge-coupled device imagers," Optical Eng., 26, 766-772 (1987).

5. Bailey, P., C. Castelli, M. Cross, P. van Essen, A. Holland, F. Jansen, P. de Korte, D. Lumb, K. McCarthy, P. Pool and P. Verhoeve, "Soft x-ray performance of back-illuminated EEV CCDs," in *EUV, X-ray and Gamma Ray Instrumentation for Astronomy and Atomic Physics*, Proc. SPIE 1384, (1990).

6. Janesick , J.R., T. Elliott, T. Daud, J. McCarthy and M.M. Blouke, "Backside charging of the CCD,' in *Solid State Imaging Arrays* (Eds. K.N. Prettyjohns and E.L. Dereniak), Proc. SPIE 570, 46-79 (1985).

7. Bosiers, J.T., N.S. Saks, D. McCarthy, M.C. Peckerar and D.J. Michels, "CCDs for high resolution imaging in the near and far UV," in *Ultraviolet Technology* (Ed. R.E. Huffman), Proc. SPIE 687, 126-135 (1986).

8. Stern, R.A., T. Whittemore, M. Winzenread and M.M. Blouke, "Ultraviolet quantum efficiency and vacuum stability of ion-implanted, laser annealed CCDs," in *Optical Sensors and Electronic Photography*, (Eds. M.M. Blouke and D. Pophal), Proc. SPIE 1071, 43-57 (1989).

9. Blouke, M.M., "Model of a thinned CCD," in Proc. SPIE 1439 (1990).

10. Grove, A.S., *Physics and Technology of Semiconductor Devices*, (John Wiley and Sons:New York:1967) pg. 145.

11. McKelvey, J.P., *Solid State and Semiconductor Physics* (Harper & Row:New York:1966) pg. 350.

12. Crowell, M.H. and E.F. Labuda, "The silicon diode array camera tube," Bell System Tech. J., 48, 1481-1528 (1969).